

Beyond Conventional Heating: Unlocking the Synergy Between Microwave Irradiation and pH Control for High-Efficiency Fabrication of Phyto-Copper Oxide Nanoparticles

Amal Alqahtani¹, Nesrine MR Mahmoud ¹, Suriya Rehman ², Somia B Ahmed ¹

¹Department of Basic Sciences, Deanship of Preparatory Year and Supporting Studies Imam Abdulrahman bin Faisal University, Dammam, 34212, Saudi Arabia; ²Department of Epidemic Diseases Research, Institute for Research and Medical Consultation (IRMC) Imam Abdulrahman bin Faisal University, Dammam, 34212, Saudi Arabia

Correspondence: Somia B Ahmed, Department of Basic Sciences, Deanship of Preparatory Year and Supporting Studies Imam Abdulrahman bin Faisal University, P.O. Box 1982, Dammam, 34212, Saudi Arabia, Tel +966507567250, Email sbahmed@iau.edu.sa

Introduction: Sustainable nanotechnology requires synthesis approaches that are environmentally benign while maintaining high efficiency, yield, and functionality. Plant-mediated synthesis combined with advanced heating techniques offers a promising route to achieve these goals.

Methods: Phyto-copper oxide nanoparticles (Phy-CuO-NPs) were synthesized using *Psidium guajava* leaf extract under different pH conditions via two approaches: conventional heating (Series A) and microwave-assisted synthesis (Series B). The influence of pH and heating mode on nanoparticle formation was systematically evaluated. The synthesized nanoparticles were characterized using physicochemical and morphological techniques, and their antibacterial activity was assessed against *Staphylococcus aureus* and *Pseudomonas aeruginosa*.

Results: Microwave-assisted synthesis significantly altered pH-dependent nucleation pathways, resulting in nanoparticles with enhanced crystallinity, more uniform morphology, higher copper content, and improved colloidal stability, particularly under alkaline conditions. Series B nanoparticles showed a 34% increase in maximum yield (up to 80 mg/g) while achieving a 92% reduction in energy consumption compared to the conventional method. Antibacterial assays revealed strong inhibitory activity against both tested strains, with greater efficacy against Gram-negative bacteria.

Discussion: The improved antibacterial performance is attributed to the bio-capped nature of the nanoparticles, which facilitates cellular entry and promotes intracellular copper ion release, leading predominantly to reactive oxygen species generation rather than direct ionic toxicity. This study highlights the synergistic role of microwave irradiation and pH control in enhancing both sustainability and functionality.

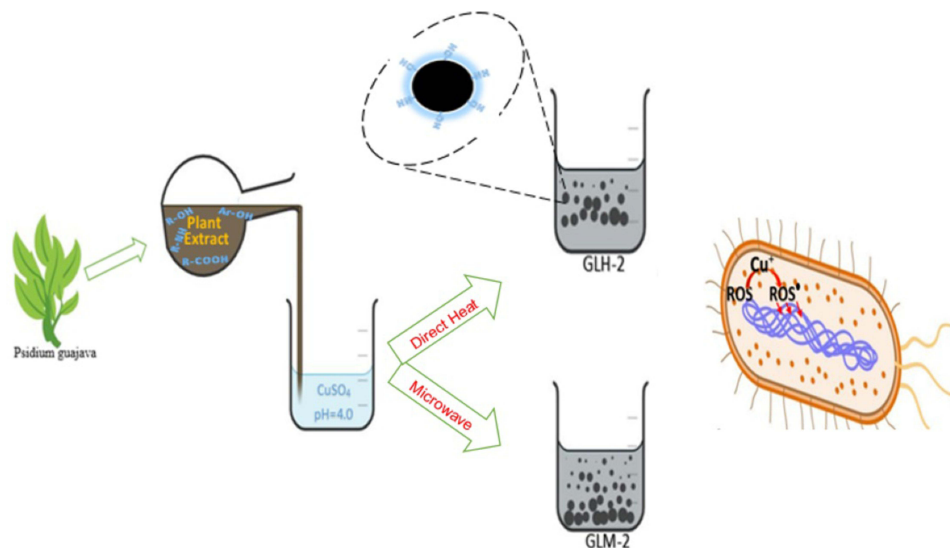
Keywords: phyto, green fabrication, biomass, valorization, microwave synthesis, copper oxide nanoparticles, antibacterial mechanism, reactive oxygen species

Introduction

The escalating global challenge of antimicrobial resistance necessitates the urgent development of novel antibacterial agents that can bypass conventional resistance mechanisms.¹ In this critical context, inorganic nanomaterials, particularly copper oxide nanoparticles (CuO-NPs), have emerged as a highly promising class of antimicrobial agents due to their broad-spectrum activity, cost-effectiveness, and remarkable chemical stability.² However, the traditional chemical synthesis of CuO-NPs often relies on toxic reducing agents and hazardous solvents, generating harmful by-products that pose significant environmental and biocompatibility concern.³ This inherent limitation has catalyzed a paradigm shift towards green synthesis methodologies, which utilize biological extracts to reduce metal ions and stabilize the resulting



Graphical Abstract



nanoparticles in a single, eco-friendly step.⁴ Agricultural waste biomass represents an abundant, renewable, and under-utilized resource for such sustainable nanomaterial production. *Psidium guajava* (guava) leaves, a widely available agricultural residue, are particularly rich in polyphenols, flavonoids, and terpenoids.⁵ These phytochemicals are not simply passive reducing agents; they actively regulate the nucleation and growth of nanoparticles, functioning as sophisticated bio-capping ligands that dictate the final size, morphology, and surface chemistry.⁶ The choice of synthesis methodology is equally critical in determining the properties of the resulting nanomaterial. While conventional heating (CH) often suffers from slow and non-uniform heat transfer—leading to polydisperse products with irregular morphologies—microwave-assisted synthesis (MAS) offers a transformative alternative.⁷ Microwave irradiation delivers energy volumetrically and instantaneously via dipole polarization and ionic conduction mechanisms. This results in rapid and uniform heating throughout the reaction mixture, promoting synchronous nucleation, minimizing Ostwald ripening, and drastically reducing reaction times, thereby aligning perfectly with the principles of green chemistry.⁸ Furthermore, microwave energy can intensify the initial extraction of bioactive compounds from the guava leaf matrix, enhancing the availability of reducing and capping agents for the subsequent nanoparticle formation process.⁹

Beyond the energy input mechanism, the pH of the reaction medium is a master variable that dictates the synthesis outcome. It profoundly influences the charge state of the biomolecules, the hydrolysis kinetics of the metal precursors, and the surface potential of the newly formed nuclei.¹⁰ For instance, an alkaline pH facilitates the deprotonation of phenolic hydroxyl groups in the plant extract, thereby enhancing their reducing power and metal-chelation ability, which often leads to the formation of smaller, more stable nanoparticles.¹¹ Despite the individual importance of these parameters, the complex interplay between solution pH and the method of energy input remains poorly understood and represents a significant knowledge gap in the optimization of green synthesis protocols.

This study systematically investigated the synergistic effects of pH and heating method on the synthesis of guava leaf-derived CuO nanoparticles, hypothesizing that microwave irradiation would not only accelerate kinetics but also optimize phytochemical functionality for enhanced nanoparticle characteristics. Through comparative analysis of conventionally and microwave-synthesized NPs across pH variations, we demonstrated three key innovations: microwave-specific heating creates a shifted pH-optimum for superior crystallinity and yield; the enhanced properties are achieved with significantly reduced energy consumption; and the antibacterial mechanism operates primarily through reactive oxygen species generation rather than conventional ion-release pathways. These findings establish a sustainable, scalable platform for producing high-efficacy biogenic nanomaterials against antimicrobial resistance.

Materials and Methods

Materials and Reagents

Copper sulfate pentahydrate ($\text{CuSO}_4 \cdot 5\text{H}_2\text{O}$) and pH adjustment buffers were obtained from S.D. Fine-Chemicals Ltd., India and used without purification. The plant material used in this study was guava (*Psidium guajava* L.) leaves obtained from a local commercial market in Egypt. The plant species was identified based on standard taxonomic descriptions and published literature¹² for *Psidium guajava* L. (family: Myrtaceae). As the material was commercially sourced and not collected directly from natural habitats, no voucher specimen was deposited in a public herbarium, and formal botanical authentication by a botanist was therefore not applicable.

Preparation of Guava Leaf Extract (GLE)

After thorough washing, eighty grams of guava leaves were immersed in 1.0 L of deionized water for 24 hours at room temperature. The mixture was filtered, and the clear filtrate (GLE) was refrigerated at 4°C and utilized as the bio-reducing agent within 48 hours.¹¹

Green Synthesis of Phyto-Copper Oxide Nanoparticles (Phy-CuO-NPs)

Series A (Conventional Hotplate Method)

We dissolved 50.0 mmol of $\text{CuSO}_4 \cdot 5\text{H}_2\text{O}$ in 50 mL solutions at different pH values (3.0, 4.0, 7.0, 9.0, and deionized water). Each solution received 100 mL of GLE added dropwise with vigorous stirring at 600rpm. The mixtures were heated on digital stirring hotplate (Model: HP 130915) maintained at 120°C for 1 hour, forming black precipitates. The products (GLH-1 to GLH-5) were collected by decantation, repeatedly washed with deionized water, and dried at 80°C overnight. All products were listed in (Table 1).

Series B (Microwave-Assisted Method)

Using identical precursor solutions to Series A, 100 mL of GLE was added directly to each 50 mL solution. The mixtures were then subjected to microwave irradiation using a domestic microwave oven (Samsung, ME731K, operational frequency: 2450 MHz) at a fixed power output of 800 Watts based on preliminary screening experiments that identified these conditions as providing maximum nanoparticle yield with favorable physicochemical characteristics. The reactions were carried out in open [eg, 250 mL] glass beakers for a continuous duration of 5 minutes. The rapid formation of a black precipitate confirmed nanoparticle synthesis. The resulting nanoparticles (GLM-1 to GLM-5) were then isolated, washed, and dried following the same protocol as Series A. All products were listed in (Table 1).

To enhance reproducibility despite the inherent limitations of a domestic microwave oven (eg, non-uniform heating and lack of real-time thermal monitoring), standardized reaction vessels and volumes were used, and the oven was

Table 1 Sample Designations and Synthesis Conditions of Phy-CuO- NPs Prepared Using GLE

Sample Description	Series A	Sample Description	Series B
Phy- CuO-NPs prepared from <i>Psidium guajava</i> leaf extract using thermal heating at pH = 3.0	GLH-1	Phy-NPs prepared from <i>Psidium guajava</i> leaf extract using microwaves at pH = 3.0	GLM-1
Phy-CuO-NPs prepared from <i>Psidium guajava</i> leaf extract using thermal heating at pH = 4.0	GLH-2	Phy-CuO-NPs prepared from <i>Psidium guajava</i> leaf extract using microwaves at pH = 4.0	GLM-2
Phy-CuO-NPs prepared from <i>Psidium guajava</i> leaf extract using thermal heating at D.W.	GLH-3	Phy-CuO-NPs prepared from <i>Psidium guajava</i> leaf extract using microwaves D.W.	GLM-3
Phy- CuO-NPs prepared from <i>Psidium guajava</i> leaf extract using thermal heating at pH = 7.0	GLH-4	Phy-CuO-NPs prepared from <i>Psidium guajava</i> leaf extract using microwaves at pH = 7.0	GLM-4
Phy-CuO-NPs prepared from <i>Psidium guajava</i> leaf extract using thermal heating at pH = 9.0	GLH-5	Phy-CuO-NPs prepared from <i>Psidium guajava</i> leaf extract using microwaves at pH = 9.0	GLM-5

operated with continuous rotation. Future studies will employ dedicated microwave reactors to allow precise temperature control, improved reproducibility, and systematic scale-up investigations.

Evaluation of Antibacterial Activity

We tested all nanoparticle samples against *Staphylococcus aureus* ATCC 43300 (Gram-positive) and *Pseudomonas aeruginosa* ATCC 27853 (Gram-negative) using broth dilution methods.¹³ Bacterial inocula were standardized to approximately 10^7 CFU/mL. The Minimum Inhibitory Concentration (MIC) represented the lowest nanoparticle concentration preventing visible growth after incubation. The Minimum Bactericidal Concentration (MBC) was determined by sub-culturing from clear wells onto fresh agar plates, with MBC defined as the lowest concentration producing no colony growth or fewer than three colonies.

Results and Discussion

Phytochemical Capping and Functional Group Analysis (FT-IR)

Figure 1, presents the FTIR spectra of Phy-CuO nanoparticles synthesized via hotplate (Series A) and microwave irradiation (Series B). The FTIR profiles of (Figure 1a) Series A were largely similar across all samples, showing four characteristic regions. A broad band around 3500 cm^{-1} suggests the presence of O–H stretching from alcohols or phenolic compounds. A prominent peak near 1600 cm^{-1} corresponds to the C=O stretching of amide groups, while a sharp peak at 1037 cm^{-1} indicates C–O–C (ether) linkages. Finally, a distinct band at $\sim 600\text{ cm}^{-1}$ confirms the presence of Cu–O vibrations, consistent with CuO formation.¹¹ In contrast, the FTIR spectra of Series B (Figure 1b) exhibited more well-defined and intense peaks, suggesting stronger interaction between the CuO surface and phytochemicals in guava leaf extract. A broad O–H band was observed at 3400 cm^{-1} , alongside multiple well-resolved peaks at ~ 1602 , 1450 , and 1360 cm^{-1} , corresponding to C=O of amide, N–H, and N–O functionalities, respectively. Peaks in the $1050\text{--}1100\text{ cm}^{-1}$ range suggest ether, alcohol, or glycoside groups, indicating diverse plant-derived organic compounds. Additionally, the emergence of C–H stretching bands in the $850\text{--}770\text{ cm}^{-1}$ range was notable in higher pH samples (GLM-3–GLM-5), specifically GLM-5, reflecting alkane groups. All Series B samples consistently showed a Cu–O vibration band in the range ~ 611 to 700 cm^{-1} , confirming CuO formation.^{14,15} The presence of various functional groups

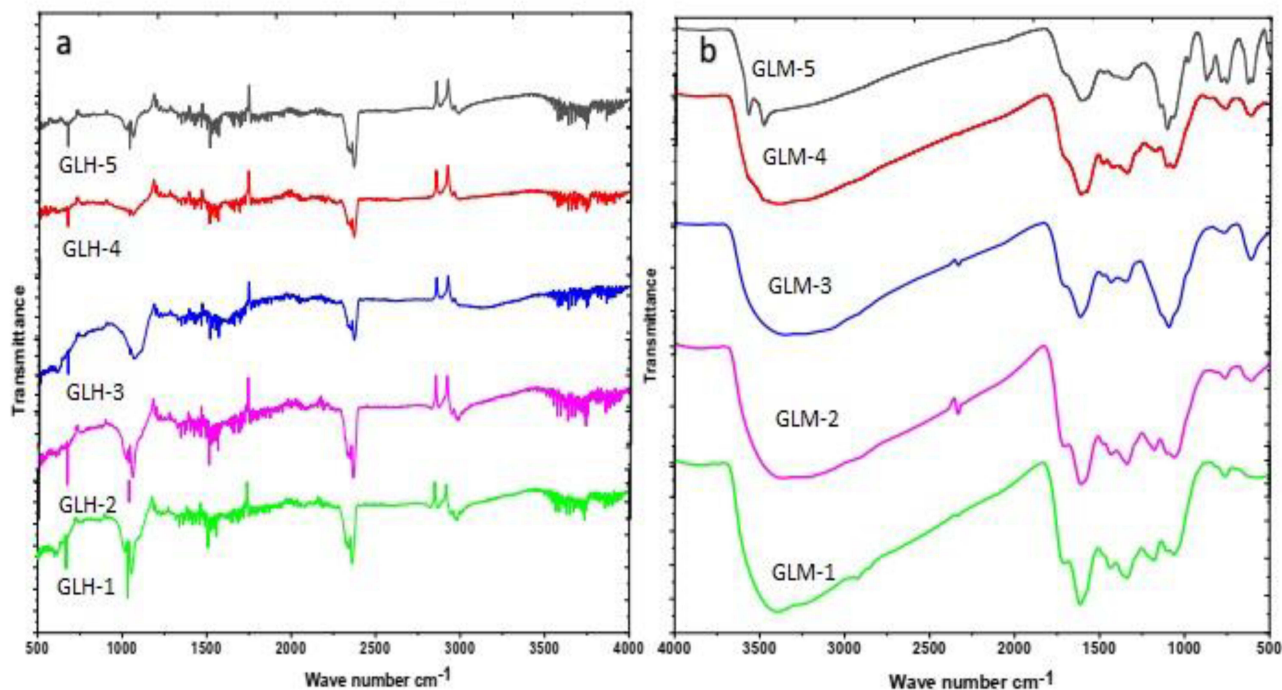


Figure 1 FT-IR of series A (a) and series B (b).

across all samples clearly indicates the bio-capping of organic residues surrounding the biosynthesized CuO nanoparticles. This distinct signature enables straightforward identification of the nanoparticles as *Psidium guajava*-derived Phy-CuO-NPs.

Morphological and Structural Insights (SEM, TEM & XRD)

Figure 2 presents the surface morphology of the samples under investigation (Series A and B). The SEM micrographs of Series A (GLH-1 to GLH-5), shown in Figure 2, reveal non-uniform surfaces composed of aggregated and compact layers of CuO nanoparticles. GLH-1 and GLH-3 exhibit highly compact morphologies, suggesting denser particle agglomeration and limited visible surface irregularities. In contrast, GLH-4 and GLH-5 display rougher and more heterogeneous surface textures, indicative of looser packing and the presence of surface features that may favor increased interfacial interactions. GLH-2 shows a relatively homogeneous morphology with moderate surface roughness, which may contribute to enhanced surface interactions. On the other hand, the SEM images of Series B (GLM-1 to GLM-5), displayed in Figure 2, show a remarkably more homogeneous and finely dispersed surface morphology compared to Series A. The particles are uniformly distributed across the substrate with significantly reduced agglomeration. GLM-1 and GLM-3 exhibit smooth surfaces with dense nanoparticle coverage, while GLM-2, GLM-4, and GLM-5 show highly uniform and evenly spaced nanoparticles, forming a well-structured, porous layer. This profound difference underscores the advantage of microwave radiation in achieving superior morphological control. The volumetric and uniform heating characteristic of microwave irradiation minimizes localized superheating and temperature gradients, which are common

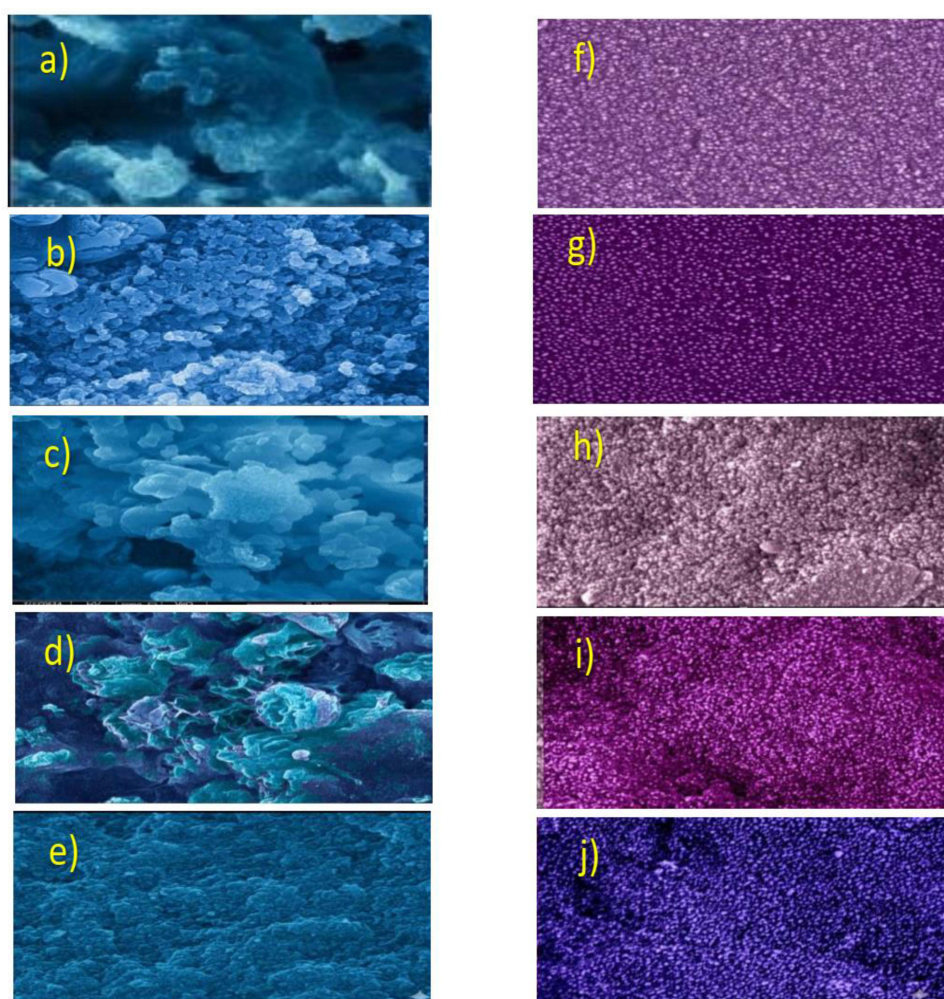


Figure 2 SEM of series A: (a) GLH-1 (b) GLH-2 (c) GLH-3 (d) GLH-4 (e) GLH-5 and SEM of series B: (f) GLM-1 (g) GLM-2 (h) GLM-3 (i) GLM-4 (j) GLM-5.

in conventional heating. This uniform energy distribution promotes simultaneous nucleation throughout the reaction volume and ensures a more controlled and even growth of nanoparticles.¹⁶ The rapid heating rates achieved by microwave radiation also contribute to faster nucleation kinetics, leading to a larger number of smaller nuclei that grow uniformly, resulting in the observed fine dispersion and reduced clustering. The ability of microwave radiation to provide such precise control over the reaction environment is a key factor in producing nanomaterials with tailored morphological properties.¹⁷ The precise control offered by microwave-assisted synthesis plays a crucial role in tailoring the morphological features of the resulting nanomaterials. Furthermore, these morphological differences are influenced by variations in the pH of the reaction medium as well as by the capping interactions of phytochemicals derived from *Psidium guajava* leaf extract with the nanoparticle surfaces.

Based on TEM analysis, Series A nanoparticles exhibit average particle sizes within the range of 5.7–16.8 nm, while Series B nanoparticles show average sizes ranging from 3.9–14.3 nm. Additionally, both series display a consistent trend of decreasing average particle size with increasing pH. All TEM analysis figures are provided in [Supplementary Figure 1](#).

Figure 3 presents the X-ray diffraction (XRD) patterns of two CuO nanoparticle series synthesized using *Psidium guajava*-derived leaf extract under varying pH conditions and heating methods: microwave-assisted (GLM-1–GLM-5) **Figure 3a** and hotplate-assisted (GLH-1–GLH-5). In the microwave-assisted series (GLM-1–GLM-5) **Figure 3b**, a progressive improvement in crystallinity and CuO phase definition was observed as the pH increased. At acidic pH values and in distilled water with no adjustment (pH 3 and 4, GLM-1, GLM-2 and GLM-3), the XRD signals were extremely weak and diffuse, indicating poor crystallinity. This is likely due to hindered reduction of Cu^{2+} and weak complexation with protonated plant biomolecules, resulting in sluggish nucleation and the formation of amorphous or ultra-fine particles.¹¹ Near-neutral conditions (pH 7, GLM-4) yielded moderately crystalline CuO, while the basic environment (pH 9, GLM-5) produced sharp, intense peaks corresponding to -110 , -111 and 002 planes consistent with monoclinic CuO (JCPDS 05-0661).^{8,18} This indicates that the combination of rapid microwave energy and alkaline conditions, which enhance phytochemical deprotonation and reducing power, is optimal for well-structured crystal growth. In contrast, the hotplate-synthesized series (GLH-1 to GLH-5) displayed a distinct crystallinity trend, with the most crystalline CuO nanoparticles forming unexpectedly at acidic to near-neutral pH levels (pH 3–7). Specifically,

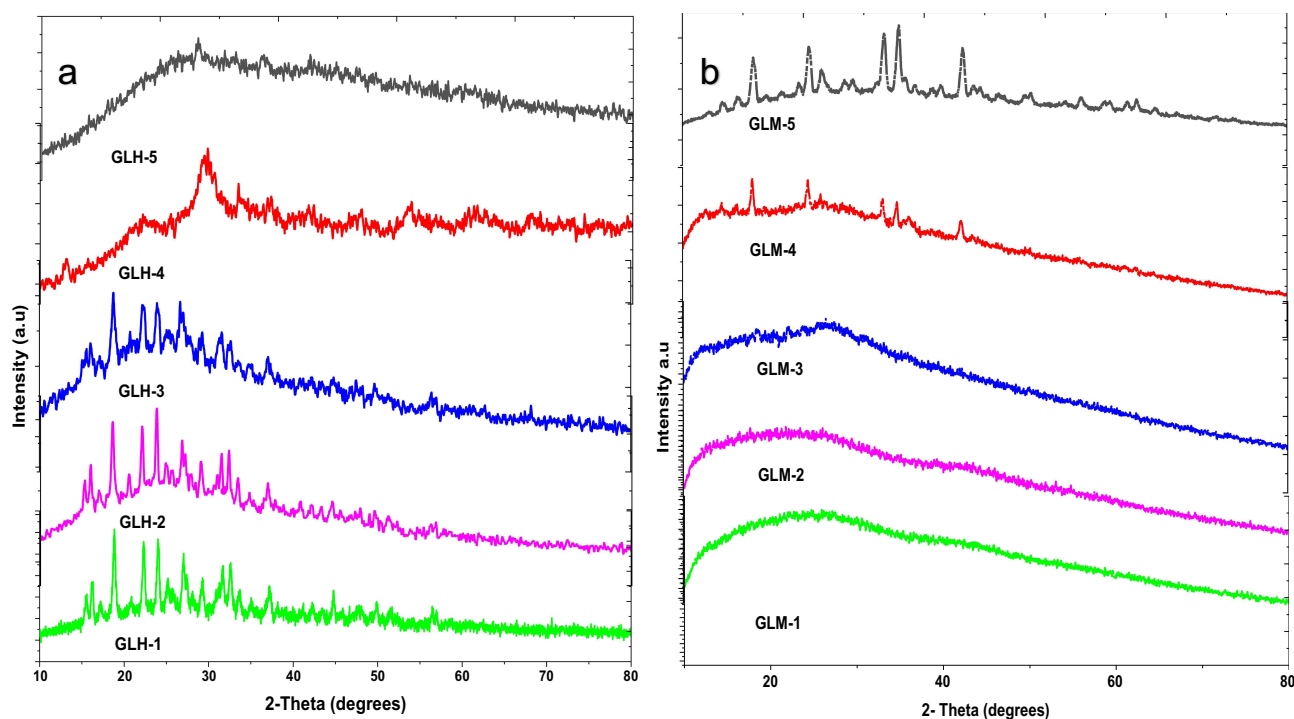


Figure 3 XRD analysis of series A (a) and series B (b).

sample GLH-1 (pH 3) exhibited the sharpest diffraction peaks, indicating the highest crystallinity, while GLH-2 and GLH-3 also showed sharp, yet less intense, peaks. All recorded peaks for these samples matched the characteristic 2 θ values for the monoclinic CuO phase (JCPDS 05–0661), corresponding to the (110), (002), and (202) planes. This suggests that under conventional heating's slow kinetics, an acidic environment optimally facilitates copper precursor hydrolysis and enhances interaction with the plant extract's active constituents and weak diffraction peaks implied poor crystallinity, likely due to over-stabilization by strongly deprotonated phytochemicals that prevent proper growth of CuO nuclei. These findings clearly demonstrate that the optimal pH for high crystallinity is not universal but is intrinsically linked to the heating method. Microwave-assisted synthesis favors basic conditions, where rapid, volumetric heating synergizes with the enhanced reactivity of deprotonated phytochemicals. Conversely, conventional heating achieves its best crystallinity under acidic conditions, where slower thermal input allows for controlled precursor hydrolysis and interaction. Understanding this synergistic interplay is critical for rationally optimizing green synthesis protocols to tailor nanoparticle structure for specific applications, such as antibacterial agents.

Elemental Composition and Colloidal Stability (EDX & Zeta Potential)

The EDX and Zeta Potential data provide critical, interconnected insights that go beyond mere composition and stability, revealing a fundamental difference in the nature of the nanoparticles produced by the two synthesis methods. This difference can be conceptualized as a variation in the “core-shell” model, where the “core” is the inorganic CuO and the “shell” is the organic phytochemical capping layer.

The EDX results (Table 2) reveal a stark contrast in synthesis efficiency and product purity. In Series A (conventional heating), the copper content is not only lower but also highly erratic, showing no clear correlation with pH. For instance, GLH-1 (pH 3) and GLH-3 (D.W.) exhibit remarkably low Cu Percentages (7.12% and 4.90%, respectively) coupled with high carbon content (~46% and ~36%). This indicates a nanoparticle that is heavily encapsulated by unreacted or loosely bound organic residues from the guava leaf extract.¹¹ The slow, non-uniform heating of the conventional method appears to favor the adsorption and co-precipitation of organic matter over the efficient reduction and incorporation of copper ions into a crystalline lattice, a finding corroborated by the poor and variable crystallinity observed in the XRD data for this series. In opposite contrast, Series B (microwave-assisted) demonstrates a paradigm of enhanced control and efficiency. The microwave-synthesized nanoparticles exhibit a clear, ascending trend in copper content with increasing pH, culminating in GLM-4 (pH 7) with a Cu content of 21.06%—significantly higher than any sample in Series A. Concurrently, the carbon content in Series B is generally lower and shows a more predictable trend. This is a direct consequence of the microwave's volumetric heating. The rapid and uniform energy delivery dramatically accelerates the reduction kinetics of Cu²⁺ ions, promoting a more complete conversion to CuO.¹⁹ Furthermore, the intense local heating likely leads to a more controlled and dense packing of the phytochemical capping agents, forming a thinner, more effective shell around a larger, purer inorganic core.¹⁷ This explains the superior crystallinity observed in the XRD patterns for Series B at higher pH, as a purer core is more amenable to well-ordered crystal growth.

The zeta potential measurements (Table 2) directly complement the EDX findings and provide a mechanistic explanation for the morphological and antibacterial results. The surface charge of Series A is moderately negative and inconsistent, reflecting the irregular and likely heterogeneous organic coating suggested by the erratic EDX data.

Table 2 Zeta Potential Values of CuO-NPs from Series A and B

Series A	Zeta Potential Values (mv)	Series B	Zeta Potential Values (mv)
GLH-1	−12.5	GLM-1	−23.41
GLH-2	−1.25	GLM-2	−3.8
GLH-3	−12.40	GLM-3	−13.84
GLH-4	−6.18	GLM-4	−13.72
GLH-5	−6.72	GLM-5	−7.83

Series B, however, displays a profoundly different surface character. The zeta potentials are consistently more negative, with GLM-1 reaching -23.41 mV. This strongly suggests a surface densely functionalized with anionic groups from the guava phytochemicals, such as deprotonated phenols and carboxylates. This finding is in perfect agreement with the more intense and well-defined functional group peaks observed in the FT-IR spectra for Series B. The resulting strong electrostatic repulsion between nanoparticles is the primary reason for the remarkably homogeneous, non-aggregated morphology witnessed in the SEM images. This enhanced colloidal stability is not just a material property; it has direct biological relevance. A well-dispersed nanoparticle suspension presents a higher effective surface area for interaction with bacterial cells, potentially enhancing antibacterial efficacy.¹⁹

Synthesis Yield of Phy-CuO-NPs

The newly fabricated PYS-CuO-NP yield depended strongly on both pH and synthesis method. The yields of all samples from Series A and B were measured in mg/g and are presented in (Table 3 and Figure 4). The effects of the preparation medium's pH and the use of microwave-assisted synthesis were evaluated. Both parameters had a notable influence on the yield. Increasing the pH from 3.0 to 9.0 resulted in a sharp rise in yield for both series. For Series A, the yield increased from 12.8 mg/g at pH 3.0 to 50.8 mg/g at pH 9.0, while Series B rose from 13.6 mg/g to a maximum of 80 mg/g over the same pH range. Although both series followed the same yield trend, Series B consistently produced higher yields than Series A. Microwave irradiation significantly enhanced the yield across all pH values—by about 6% at pH 3.0, increasing gradually to 34% at pH 9.0. The highest yield of *Psidium guajava*-derived CuO-NPs was achieved under neutral to slightly alkaline conditions using microwave heating rather than conventional electric heating. This can be attributed to the higher concentration of hydroxyl groups in neutral to alkaline media, which promotes the precipitation of copper ions as copper hydroxide, subsequently transforming into CuO upon heating. The improvement observed with microwave irradiation is likely due to its ability to heat the reaction mixture both internally and externally, thereby increasing the frequency of collisions between reactant molecules. The yields for both series increased with rising pH, but Series B consistently surpassed Series A, reaching a maximum yield of 80 mg/g at pH 9 which 34% improvement over conventional methods. This enhancement attributes to rapid, uniform microwave heating that increases molecular collision frequency and ensures more complete reactions.²⁰ The microwave approach provided dramatic energy efficiency advantages. The 5-minute microwave process consumed approximately 0.083 kWh, twelve times less energy than the 1-hour conventional method (1 kWh). This combination of higher yield and lower energy input positions microwave-assisted synthesis as a clearly superior, sustainable platform for scalable nanomaterial production.²¹

Antibacterial Activity: Efficacy, Selectivity, and Structure-Activity Relationships

The antibacterial evaluation of the phyto-synthesized CuO-NPs revealed a complex interplay between synthesis method, nanoparticle composition, and biological activity against Gram-positive and Gram-negative pathogens. The quantitative MIC/MBC data, coupled with the visual evidence from the agar plates (Figures 5 and 6), demonstrate not only potent antibacterial effects but also clear structure-activity relationships that illuminate the underlying mechanism.

Table 3 Comparison of CuO-NPs' Yields (mg/g) for Series A and Series B

Series A	Yield (mg/g)	Series B	Yield (mg/g)	Difference %
GLH-1	12.8	GLM-1	13.6	5.9%
GLH-2	18.4	GLM-2	20.0	8.0%
GLH-3	32.0	GLM-3	36.8	13.0%
GLH-4	40.0	GLM-4	49.6	19.3%
GLH-5	52.8	GLM-5	80.0	34.0%

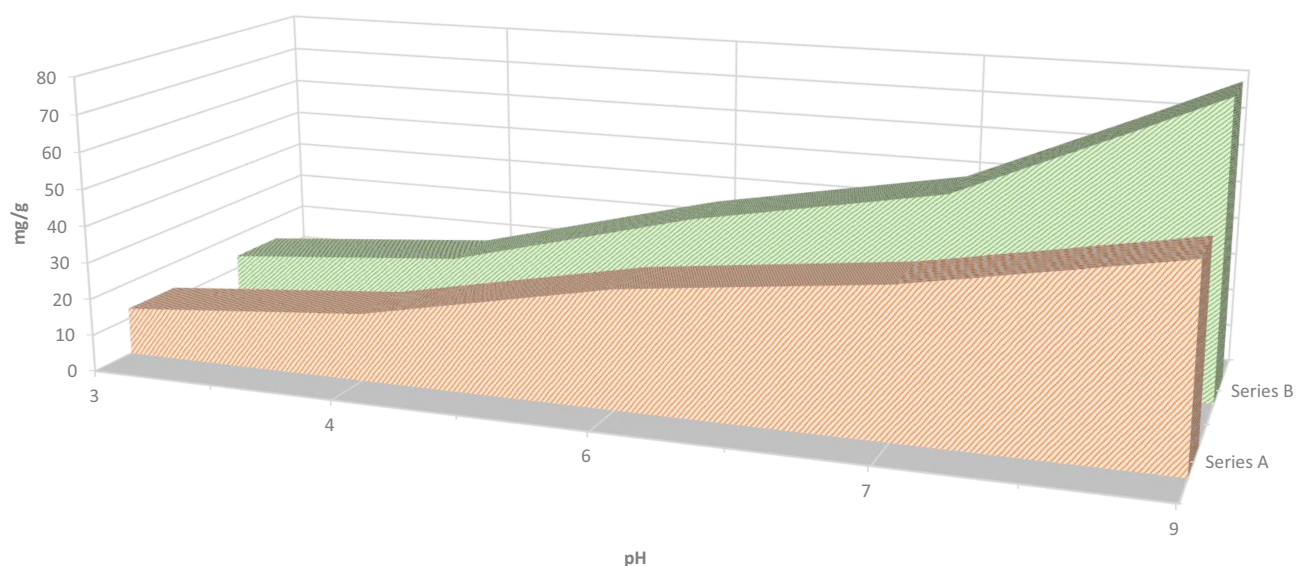


Figure 4 The yield changes of series A and series B.

Staphylococcus aureus

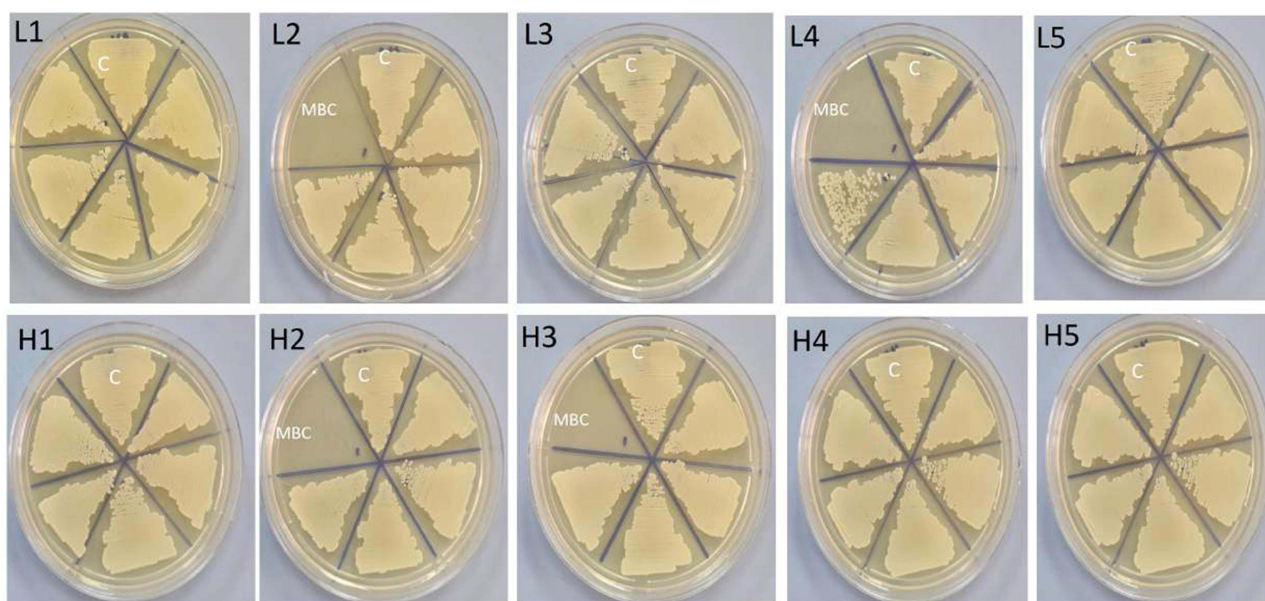


Figure 5 Agar plates representing the MBC (Minimum Bactericidal Concentration) of series series B and series A ranging in the concentration from 1 to 16 mg/mL from right to left, C represents the control (untreated cells) against *S. aureus*.

A key finding is the consistent and significant selectivity towards the Gram-negative bacterium, *Pseudomonas aeruginosa*. For instance, samples from both Series A (GLH-2, GLH-3) and Series B (GLM-1, GLM-4, GLM-5) achieved complete (100%) bacterial elimination of *P. aeruginosa* at 16 mg/mL, with some (GLM-4, GLM-5) showing high efficacy (70–90%) starting at just 8 mg/mL. In contrast, activity against the Gram-positive *Staphylococcus aureus* was generally lower, with only a few samples (GLH-2, GLH-3, GLM-2, GLM-5) achieving complete eradication at the highest concentration. This differential susceptibility aligns with established literature on metal oxide nanoparticles and is fundamentally rooted in cell wall architecture.²² The thin, porous peptidoglycan layer overlain by a complex outer membrane in Gram-negative bacteria

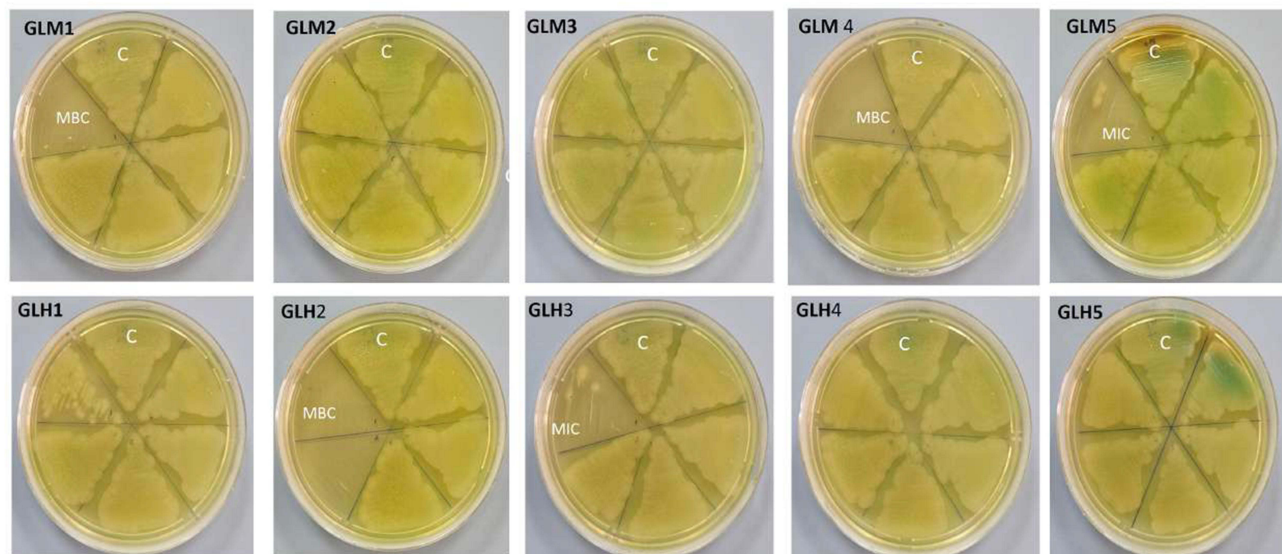
Pseudomonas aeruginosa

Figure 6 Agar plates representing the MBC (Minimum Bactericidal Concentration) of series B and series A ranging in the concentration from 1 to 16 mg/mL from right to left, C represents the control (untreated cells) against *P. aeruginosa*.

like *P. aeruginosa* is more susceptible to nanoparticle-induced disruption and penetration compared to the thick, multi-layered peptidoglycan structure of Gram-positive cells.^{23,24}

The performance of Series A samples revealed an intriguing relationship between composition and activity. GLH-2 (pH 4) and GLH-3 (D.W.) demonstrated complete termination of *P. aeruginosa* at 16 mg/mL, while GLH-1 (pH 3) showed approximately 70% efficacy. Against *S. aureus*, the antibacterial activity was generally reduced, with only GLH-2, GLH-3, and GLM-2 (pH 4) achieving complete elimination at the highest concentration tested. The exceptional performance of GLH-2 is particularly noteworthy given its relatively low copper content (4.41%) and moderate surface charge (−1.25 mV). This suggests that factors beyond mere metal content, potentially including the specific arrangement and composition of the phytochemical capping layer as indicated by its balanced carbon and oxygen content, play a crucial role in determining antibacterial efficacy. Series B nanoparticles, synthesized via microwave assistance, generally showed improved and more consistent antibacterial profiles. GLM-5 (pH 9) demonstrated 90% efficacy against *S. aureus* at 8 mg/mL, reaching 100% at the higher concentration. This enhanced performance correlates with the superior physical characteristics of microwave-synthesized nanoparticles observed in characterization studies, including higher copper purity and more stable surface properties.²⁵

Proposed Antibacterial Mechanism Phy-CuO-NPs Against Both Gram-Positive and Gram-Negative Bacteria

Based on our integrated characterization data, we propose a refined, multi-stage mechanism for these Phy-CuO-NPs' antibacterial action.²⁶ The initial step of the antibacterial mechanism is the penetration of the biogenic CuO nanoparticles through the bacterial cell wall.^{27–29} Based on our FT-IR and zeta potential data, the organic residues on the nanoparticle surface and its overall negative charge are key properties that facilitate this entry. Once the nanoparticles are inside the bacterial cell, they enhance the production of damaging reactive oxygen species (ROS), thereby initiating the process of cell damage. The subsequent step involves the liberation of copper ions from the biogenic CuO nanoparticles inside the bacterial cell. These copper ions then directly catalyze the formation of destructive ROS. The ultimate elimination of bacteria is proposed to occur through two synchronized pathways. Pathway I: The copper ions directly bind to essential cellular components, thereby deactivating catalytic process and metabolic processes. Pathway II: The newly generated ROS attack directly the cell organism and cause severe oxidative stress to cellular organelles, leading to irreparable

damage such as DNA fragmentation, lipid peroxidation, and enzyme degradation. Based on the results from our antibacterial investigation, the strong performance of the GLH-2 phase may point toward Pathway II as a possible dominant mechanism, potentially linked to ROS-mediated damage, which could be influenced by its low copper content, as determined by EDX analysis, reinforces this conclusion, implying that the copper ions serve a crucial role as a trigger for ROS activation rather than as a bulk antimicrobial agent.

Conclusion

This study successfully demonstrates an innovative and efficient strategy for the biosynthesis of two active series A&B based on Phy-CuO-NPs by valorizing *Psidium guajava* leaf biomass. The work unequivocally establishes that microwave-assisted synthesis (MAS) fundamentally outperforms conventional heating, not merely as a faster alternative, but as a method that change the fundamental nucleation and growth pathways. One can listed that in the following point. First, Superior Material Properties: MAS produced CuO-NPs with enhanced crystallinity (under alkaline pH), a uniform and dispersed morphology, higher elemental purity, and superior colloidal stability compared to conventionally synthesized nanoparticles. Second, Process Efficiency and Scalability: The microwave approach achieved a 34% higher maximum yield (80 mg/g) while reducing energy consumption by 92%, addressing two major bottlenecks in the green synthesis of nanomaterials yield and energy cost. Third, Refined Antibacterial Mechanism: the study provides compelling evidence that the antibacterial action is predominantly mediated by a ROS-driven oxidative burst catalyzed by intracellularly released copper ions, a mechanism that is more sophisticated and potent than simple ion toxicity. Finally, this research provides a comprehensive, sustainable, and scalable paradigm for producing high-performance biogenic CuO-NPs. By intelligently coupling agricultural waste valorization with microwave process intensification, we have outlined a path forward for the economic and environmentally friendly production of nanomaterials with significant potential against antimicrobial resistance.

Author Contributions

All authors made a significant contribution to the work reported, whether that is in the conception, study design, execution, acquisition of data, analysis and interpretation, or in all these areas; took part in drafting, revising or critically reviewing the article; gave final approval of the version to be published; have agreed on the journal to which the article has been submitted; and agree to be accountable for all aspects of the work.

Disclosure

The authors report no conflicts of interest in this work.

References

1. Murugan B, Rahman D, Fatimah I, et al. Green synthesis of CuO nanoparticles for biological applications. *Inorg Chem Commun.* 2023;155:111088. doi:10.1016/j.inoche.2023.111088
2. Nejo AO, Adetona AJ, Lawal A. Green synthesis of nickel oxide nanoparticles and its application in the degradation of methyl red. *Lafia J Sci Ind Res.* 2024;2(2):54–60. doi:10.62050/ljsir2024.v2n2.328
3. Mahmoud NMR, Elbadawy HA, Refaat HM. An efficient green protocol for photo-degradation of bromophenol blue dye. *Desalin Water Treat.* 2021;229:403–412. doi:10.5004/dwt.2021.27384
4. Bhardwaj R, Naruka D, Kapoor N, Gambhir L. Green synthesis and antibacterial potency of Ag/CuO/ZnO nanoparticles derived from *Psidium guajava* L. extracts. *Plant Sci Today.* 2024;11(4):314–322. doi:10.14719/pst.3221
5. Alnaddaf LM, Almuhammady AK, Salem KFM, Alloosh MT, Saleh MM, Al-Khayri JM. Green synthesis of nanoparticles using different plant extracts and their characterizations. In: Al-Khayri JM, Ansari MI, Singh AK, editors. *Nanobiotechnology: Mitigation of Abiotic Stress in Plants.* Springer International Publishing; 2021:165–199. doi:10.1007/978-3-030-73606-4_8
6. Gabano E, Ravera M. Microwave-assisted synthesis: can transition metal complexes take advantage of this green method? *Molecules.* 2022;27(13):1–38. doi:10.3390/molecules27134249
7. Rosa R, Ponzoni C, Leonelli C. Direct energy supply to the reaction mixture during microwave-assisted hydrothermal and combustion synthesis of inorganic materials. *Inorganics.* 2014;2(2):191–210. doi:10.3390/inorganics2020191
8. Zayyoun N, Bahmad L, Laânab L, Jaber B. The effect of pH on the synthesis of stable Cu₂O/CuO nanoparticles by sol–gel method in a glycolic medium. *Appl Phys A.* 2016;122(5):1–7. doi:10.1007/s00339-016-0024-9
9. Messai Y, Bouarroudj T, Chetoui A, et al. Correlating pH-controlled green synthesis of NiO nanoparticles with their magnetic properties and catalytic performance. *Mater Today Commun.* 2023;37:107530. doi:10.1016/j.mtcomm.2023.107530
10. Huynh HD, Nargotra P, Wang HMD, Shieh CJ, Liu YC, Kuo CH. Bioactive compounds from guava leaves (*Psidium guajava* L.): characterization, biological activity, synergistic effects, and technological applications. *Molecules.* 2025;30(6):1278. doi:10.3390/molecules30061278

11. Mahmoud NMR, Al-otaibi AL, Akhtar S, et al. Study the effect of simple extraction techniques to synthesizing promising antimicrobial bio-capped copper oxide nanoparticles. *Green Chem Lett Rev.* 2023;16(1):1–15. doi:10.1080/17518253.2023.2260417
12. Bussmann R, Zambrana N, Njoroge G. Psidium guajava L. Myrtaceae. In: *Ethnobotany of the Mountain Regions of Africa.* 2020:1–5. doi:10.1007/978-3-319-77086-4_130-1
13. Rehman S, Albhishiri G, Alsalem Z, et al. Bionanocomposites comprising mesoporous metal organic framework (ZIF-8) phytofabricated with *Allium sativum* as alternative nanomaterials to combat antimicrobial drug resistance. *Bioprocess Biosyst Eng.* 2024;47(8):1335–1344.
14. Ali LM, Hassan HE, El-Raie AE, Ahmed AERA, Saleh SS. The prospect of using guava leaf extract for biosynthesizing chitosan nanoparticles. *Adv Nat Sci Nanosci Nanotechnol.* 2019;10(4):45005. doi:10.1088/2043-6254/ab4804
15. Somchaidee P, Tedsree K. Green synthesis of high dispersion and narrow size distribution of zero-valent iron nanoparticles using guava leaf (*Psidium guajava* L) extract. *Adv Nat Sci Nanosci Nanotechnol.* 2018;9:35006. doi:10.1088/2043-6254/aad5d7
16. Chandrasekaran S, Ramanathan S, Basak T. Microwave material processing-a review. *AiChE J.* 2012;58(2):330–363. doi:10.1002/aic.12766
17. Chikan V, McLaurin EJ. Rapid nanoparticle synthesis by magnetic and microwave heating. *Nanomaterials.* 2016;6(5):85. doi:10.3390/nano6050085
18. Ikhsanudin MN, Al Ichwan AR, Kuncoro DD, Muthi ASG, Jamaluddin A, Purwanto A. Cu-foil modification for anode-free lithium-ion battery from electronic cable waste. *Open Eng.* 2022;12(1):394–400. doi:10.1515/eng-2022-0041
19. Muthuvel A, Jothibas M, Manoharan C. Synthesis of copper oxide nanoparticles by chemical and biogenic methods: photocatalytic degradation and in vitro antioxidant activity. *Nanotechnol Environ Eng.* 2020;5(2):14. doi:10.1007/s41204-020-00078-w
20. Driowya M, Saber A, Marzag H, Demange L, Bougrin K, Benhida R. Microwave-Assisted Syntheses of Bioactive. *Molecules.* 2016;21:1032. doi:10.3390/molecules21081032
21. Makul N, Rattanadecho P, Agrawal DK. Applications of microwave energy in cement and concrete – a review. *Renew Sustain Energy Rev.* 2014;37:715–733. doi:10.1016/j.rser.2014.05.054
22. Babu A, Antony R. Green synthesis of silver doped nano metal oxides of zinc & copper for antibacterial properties, adsorption, catalytic hydrogenation & photodegradation of aromatics. *J Environ Chem Eng.* 2018;7(1):102840. doi:10.1016/j.jece.2018.102840
23. Shende S, Ingle A, Gade A. Green synthesis of copper nanoparticles by *Citrus medica* Linn. (Idilimbu) juice and its antimicrobial activity. *World J Microbiol Biotechnol.* 2015. doi:10.1007/s11274-015-1840-3
24. Govindasamy S, Thirumarimurugan M, Sivakumar VM. Optical, catalytic and antibacterial properties of phytofabricated CuO nanoparticles using *Tecoma castanifolia* leaf extract. *Optik.* 2016;127:7822–7828. doi:10.1016/j.ijleo.2016.05.142
25. Ali K, Ahmed B, Ansari SM, et al. Comparative in situ ROS mediated killing of bacteria with bulk analogue, Eucalyptus leaf extract (ELE)-capped and bare surface copper oxide nanoparticles. *Mater Sci Eng.* 2019;100:747–758.
26. Caroling G, Priyadarshini MN, Vinodhini E, Ranjitham AM, Shanthi P. Biosynthesis of copper nanoparticles using aqueous guava extract-characterisation and study of antibacterial effects. *Int J Pharm Biol Sci.* 2015;5(2):2230–7605.
27. Mahmoud N, Mohamed HI, Ahmed SB, Akhtar S. Efficient biosynthesis of CuO nanoparticles with potential cytotoxic activity. *Chem Pap.* 2020;74:2825–2835.
28. Reddy ARN, Lonkala S. In vitro evaluation of copper oxide nanoparticle-induced cytotoxicity and oxidative stress using human embryonic kidney cells. *Toxicol Ind Health.* 2019;35(2):159–164. doi:10.1177/0748233718819371
29. Mammari N, Lamouroux E, Boudier A, Duval RE. Current knowledge on the oxidative-stress-mediated antimicrobial properties of metal-based nanoparticles. *Microorganisms.* 2022;10(2):437. doi:10.3390/microorganisms10020437

Nanotechnology, Science and Applications

Publish your work in this journal

Nanotechnology, Science and Applications is an international, peer-reviewed, open access journal that focuses on the science of nanotechnology in a wide range of industrial and academic applications. It is characterized by the rapid reporting across all sectors, including engineering, optics, bio-medicine, cosmetics, textiles, resource sustainability and science. Applied research into nano-materials, particles, nano-structures and fabrication, diagnostics and analytics, drug delivery and toxicology constitute the primary direction of the journal. The manuscript management system is completely online and includes a very quick and fair peer-review system, which is all easy to use. Visit <http://www.dovepress.com/testimonials.php> to read real quotes from published authors.

Submit your manuscript here: <https://www.dovepress.com/nanotechnology-science-and-applications-journal>

Dovepress
Taylor & Francis Group